

# A novel miniaturized radiometer front-end for early breast cancer detection using ultra-wideband flexible antenna

Achraf Elouergui, Zakaryae Khomsi, Larbi Bellarbi, Atman Jbari

E2SN, Research Center in Sciences and Technologies of Engineering and Health, National School of Arts and Crafts, Mohammed V University in Rabat, Rabat, Morocco

## Article Info

### Article history:

Received Jan 5, 2023

Revised Jul 14, 2023

Accepted Aug 2, 2023

### Keywords:

Breast cancer

Computer simulation  
technology microwave

Flexible antenna

Miniature radiometer

Tumor

Ultra-wideband

## ABSTRACT

This article introduces a new design of the front-end part of a passive and miniature radiometer, which has been developed to detect breast cancer at an early stage, by measuring temperature in deep mammary tissues. The design and simulation of each element of the microwave radiometer are carried out using computer simulation technology microwave (CST MWS) software. The proposed measurement system consists of a miniaturized ultra-wideband (UWB) flexible antenna operating in the S-band (2-4 GHz), a breast phantom, a low noise amplifier (LNA), a bandpass filter, and a radio frequency (RF) power detector. These components were combined with active circuits to build the front-end system using the co-simulation modules provided by the CST MWS. The method is based on the concept that the virtually created tumor increases the temperature inside the breast phantom, and to detect the abnormality, we applied the proposed radiometer front-end on breast phantom to measure the gain variation. The results demonstrated that the design of the proposed miniaturized radiometer has promising performance in terms of stability and gain variation, indeed, the difference in maximum gain  $|\Delta G_{max}|$  measured between abnormal and healthy phantom is about 0.92 dB at 2.75 GHz. This indicates its potential for detecting breast tumors.

This is an open access article under the [CC BY-SA](https://creativecommons.org/licenses/by-sa/4.0/) license.



## Corresponding Author:

Achraf Elouergui

E2SN, Research Center in Sciences and Technologies of Engineering and Health

National School of Arts and Crafts, Mohammed V University in Rabat

Av. des Forces Armées Royales, Rabat 10100, Morocco

Email: Achraf\_elouergui@um5.ac.ma

## 1. INTRODUCTION

Breast cancer represents a significant public health issue and an event of great significance in the life of women, this disease occupies first place in terms of mortality and incidence. According to statistics published in 2022 [1]. The International Agency for Research on Cancer (IARC) has estimated the number of cases of breast cancer in the last 5 years to be 2.261 million (58.5% rate), and 684,996 deaths (17.7% rate). In Morocco, its incidence continues to increase, approximately one in ten women are at risk of developing breast cancer during their lifetime [2], this is an alarming number that increases with age. Researchers have shown that screening breast cancer once every 1 to 2 years is not sufficient to detect breast cancer since patients with fast-growing breast cancer account for a quarter of all breast cancer patients, so it is appropriate to combine screening with other non-invasive investigative methods [3].

The passive breast imaging technique based on the microwave radiometer is a method that allows measuring the intensity of natural electromagnetic radiation of biological tissues of the human body, it's harmless and without danger for the patients and the medical staff, this intensity is proportional to the

temperature of the tissues [4]–[7], indeed, the change in temperature (case of thermal abnormality) is caused by an increase in the metabolism of cancer cells, the generation of specific heat in the tumor is proportional to the growth rate of the tumor. Passive microwave radiometry is a very promising technique for early breast cancer detection, which also allows the detection of fast-growing tumors first [8], [9].

The objective of this work is to model a miniature passive microwave radiometer system for the early breast cancer detection, using a flexible ultra-wideband antenna operating in the S-band, and ergonomic with the breast. The technology adopted is microstrip in order to reduce costs and achieve high performance in detecting cancer cells.

This article is organized as follows: the section 1 presents the operation principle of the microwave radiometer with theoretical studies, thereafter we presented the model of healthy and abnormality of breast phantom that was used in our study, as well as the design and simulation of the miniaturized flexible antenna and its application to the breast phantom using computer simulation technology microwave (CST MWS) software [10]. The following section 2 presents the design and simulation of the microwave radiometer front-end containing the bandpass filter, radio frequency (RF) power detector, and low noise amplifier (LNA). Section 3, describes the measurement results and interpretations of the overall microwave radiometer front-end system, and finally, in section 4, some conclusions and perspectives are proposed.

## 2. METHOD

### 2.1. Operating principle of the proposed microwave radiometer front-end

Radiometry is a non-invasive breast imaging modality [11], [12], non-toxic and relatively inexpensive, which is based on measuring the power of electromagnetic noise emitted by lossy materials using passive receivers [13]. Several studies carried out in the literature concerning the architectures of the passive microwave radiometer front-end [14]–[16], have shown that the most used is the Dicke radiometer. This type of radiometer consists of a receiving part (antenna) which allows detecting the power of the electromagnetic noise, which is related to the thermal radiation self-produced in the breast tissue, a low noise amplifier, a bandpass filter and a detector to convert RF waves to direct current (DC) signals.

Figure 1 shows a schematic a depiction of a microwave radiometer front-end, connected to a flexible antenna to measure the thermal gradient on the breast surface. The concept of microwave thermal measurement is based on Planck's law. Planck [17] showed that spectral radiation is emitted by hot bodies, he formulated an equation relating to the electromagnetic radiation of a black body, as shown in (1):

$$B(f, T) = \frac{2hf^3}{c^2} \times \frac{1}{e^{\frac{hf}{k_B T}} - 1} \quad (1)$$

Where  $c$  is the speed of light,  $h$  is Planck's constant,  $k$  is Boltzmann's constant,  $B$  is the blackbody spectral luminance,  $T$  is the temperature in (K), and  $f$  is frequency (Hz).

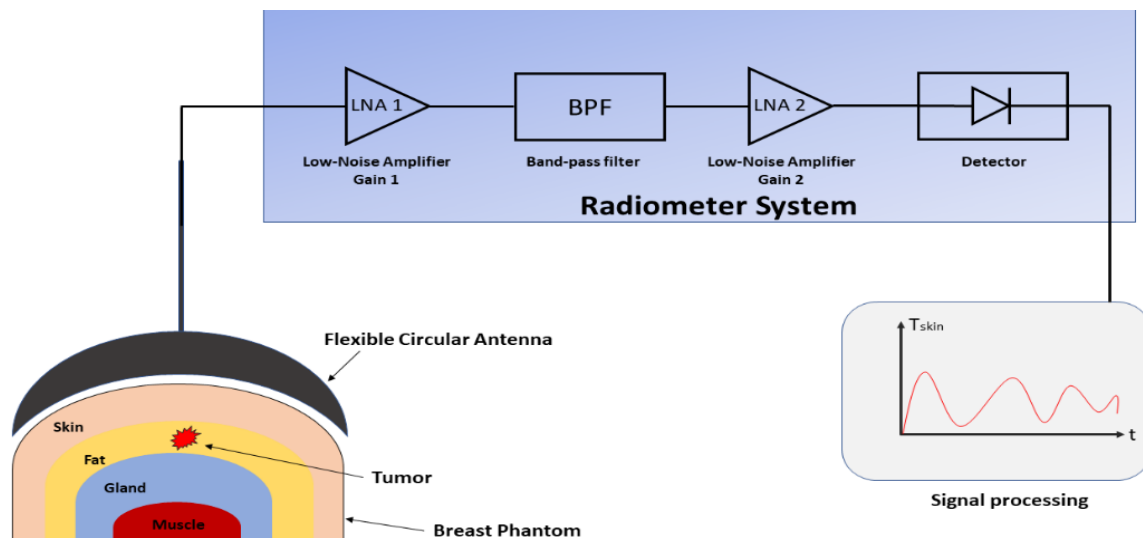


Figure 1. Block diagram of radiometer system for breast cancer detection

## 2.2. Design of the receiving part of the radiometer

### 2.2.1. Breast phantom model

According to the literature [18], [19], the structural composition of the breast has a hemispherical shape, and for its physiological characteristics consist of four essential layers, namely skin, fat, mammary gland, and muscle (see Figure 2(a)). The Figure 2(b) shows the longitudinal sectional view of the finite element grids of the breast model. The breast was modeled as a hemisphere using CST MWS software as shown in Figure 3, adhering to the physical characteristics such as the relative dielectric permittivity, the electrical conductivity chosen in the S-band, and also geometric (thickness of each breast layer and the tumor radius) as listed in the Table 1.

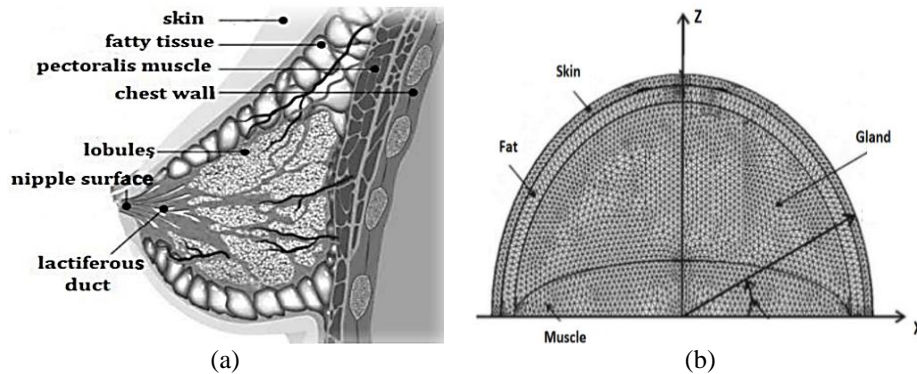


Figure 2. Breast anatomy for; (a) physiological characteristics and (b) geometric model

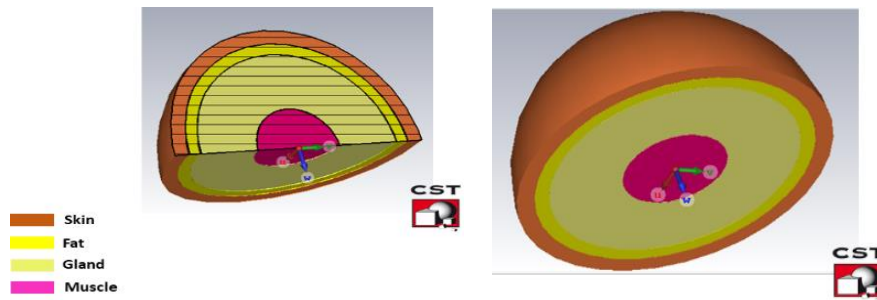


Figure 3. 3D visualization of inhomogeneous multilayer breast model using CST MWS

Table 1. Properties of the different tissue layers of the breast phantom in the S-band [20]

Phantom layers	$\epsilon_r$	Rho (Kg/m <sup>3</sup> )	Electrical conductivity (S/m)	Thickness/radius (mm)
Skin	37	1109	2.02	$E_p = 1.7$
Fat	49.4	911	2.2	$E_p = 1.4$
Gland	55.7	1041	2.93	$E_p = 7$
Muscle	51.4	1090	2.56	$E_p = 5$
Tumor	54.9	1058	4	$R = 2.5$

### 2.2.2. Microwave radiometer antenna design

In this work, the proposed patch antenna will be considered as a front-end sensor of the radiometric system that is used non-invasively and adapted to the anatomical structure of the breast, and must also ensure good contact so that antenna characteristics are not degraded. Before proceeding with antenna design, the requirements listed in the Table 2 must be respected. Based on our laboratory's research work on the antennas development [21]–[23] to benefit from previous experiences in this field, a new antenna structure has been developed for the early breast cancer detection. The antenna selected in this work is a circular, planar, flexible, miniature, ultra-wideband (UWB), and a microstrip feed, with a circle-shaped patch on the front face and a rectangular-shaped partial ground plane on the rear face. The structure shown in Figure 4 was modeled and simulated using CST MWS.

Table 2. Antenna requirements

Parameter	Requirement	Resolution
Gain	> 0 dBi	Receive low-power signals from different depths of breast tissue
Frequency	S-band	Operate with a minimum reflection coefficient
Dimension	Miniature	Easy to integrate into the screening device
Use	Contact with breast	Operate near the breast

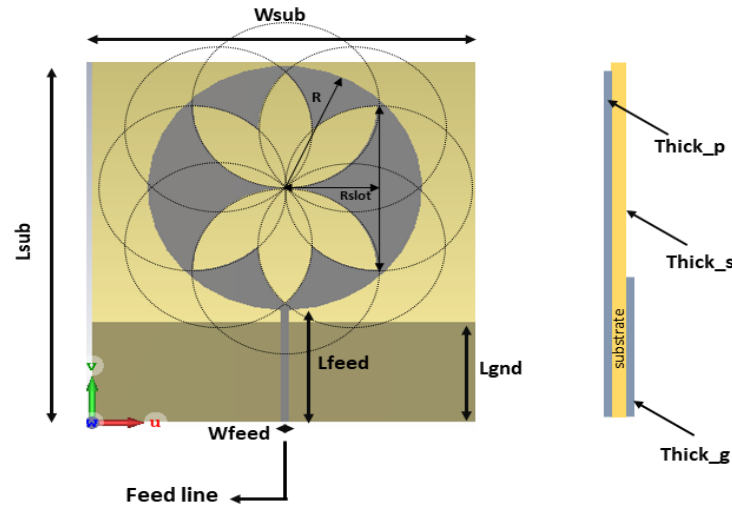


Figure 4. UWB flexible antenna design using CST MWS

The enhancement and evaluation patch antenna were carried out by numerous iterative simulations in the S-band. The choice of the S-band is justified by its good penetration of several centimeters into the breast, calculated according to the skin depth  $\delta_m$  presented in (2) [24]:

$$\delta_m = \frac{1}{\sqrt{\pi f \mu \sigma_m}} \quad (2)$$

Where  $\mu$  is the material permeability,  $\sigma_m$  is the electrical conductivity, and  $f$  is the frequency.

The Table 3 shows the different optimized parameters of the proposed flexible antenna. Kapton polyimide was chosen as the antenna substrate because of its low tangent loss factor over the entire S-band equal to 0.02, and its dielectric constant  $\epsilon_r=3.4$ .

Table 3. Proposed flexible antenna parameter values

Parameter	Thick_s	Thick_g	Thick_p	R	Rslot	Lsub	wsub	wfeed	lfeed	Lgnd
Values (mm)	0.125	0.035	0.035	9.62	6.46	28.5	27	0.6	9	7.88

From Figure 5, we observe that we have a better adaptation for a frequency band (2.3 to 6 GHz) ( $< -10$  dB), with a return loss  $S_{1,1}=-48,689$  dB for  $f_0=2.75$  GHz, and an ultra-wideband (UWB=3.67 GHz) from 2.33 GHz to 6 GHz, with a good voltage standing wave ratio (VSWR) which is equal to  $1.0084 <$  for the resonant frequency 2.75 GHz of the proposed antenna (see Figure 6), which shows the improvement of results. Figure 7 shows the radiation pattern of the proposed patch antenna.

Based on the design of the breast model using CST MWS, two approaches were studied in terms of measuring the  $S_{1,1}$  parameter of the ultra-wideband flexible antenna, the first is a phantom with tumor and the second approach is a phantom without tumor in order to analyze simulation results. From these results allowed us to conclude whether or not cancerous tumors were present. For the first scenario of the healthy breast phantom, the  $S_{1,1}$  parameter had an impact compared to the results obtained from the flexible antenna positioned in free space (see Figure 8), indeed, the resonant frequency has been changed from 2.749 GHz to 2.108 GHz with a frequency variation equal to  $|\Delta f = f_0 - f_1|=640$  MHz.

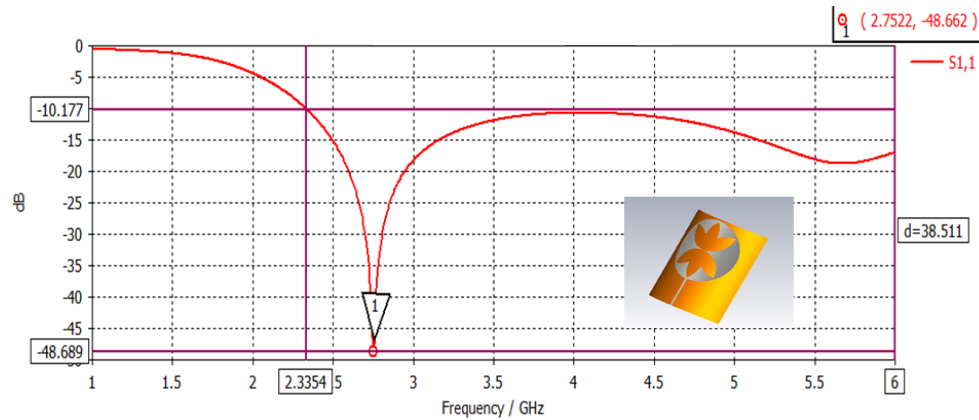


Figure 5. Coefficient S1,1 of the flexible antenna

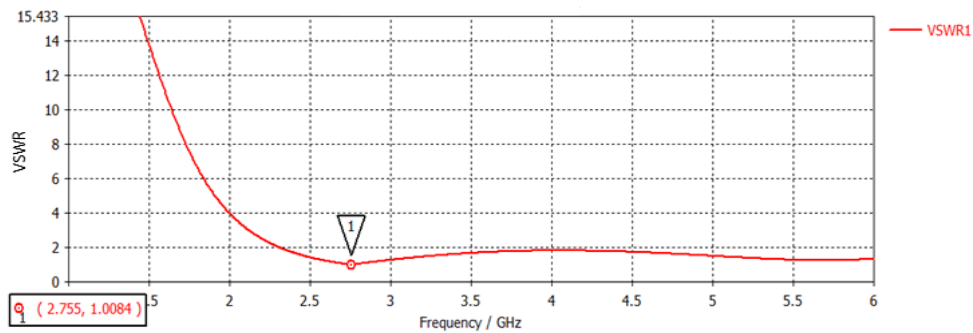


Figure 6. VSWR result of the simulated flexible antenna

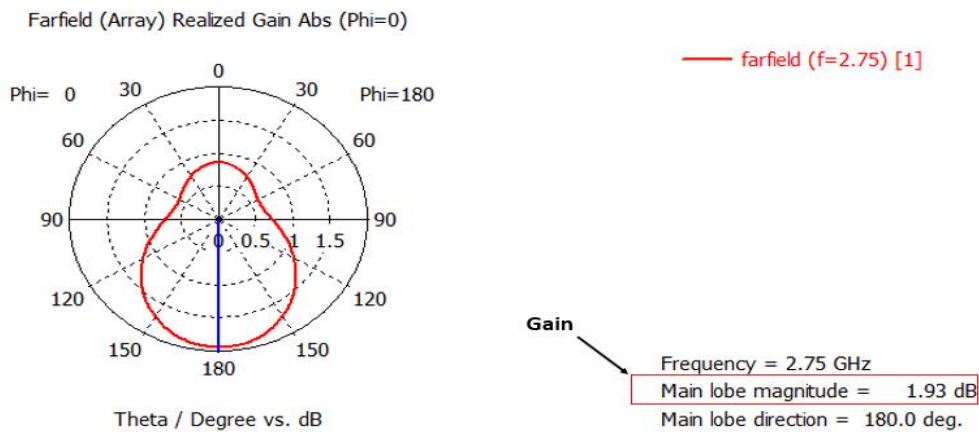


Figure 7. Radiation pattern of the flexible antenna

For the second scenario of the abnormality breast phantom, the change was rather observed in the value of the resonance frequency, indeed, the value of the said frequency varies from 2.108 GHz for the case of the flexible antenna positioned in contact with breast phantom without tumor, to 2.953 GHz for the case of the presence of the tumor, with a difference in frequency is equal to  $|\Delta f = f_2 - f_1| = 845$  MHz (see Figure 8). It can be concluded that the antenna developed in this work exhibits a very different propagation behavior from that in free space, and therefore, it can detect cancer cells in the virtually created breast phantom.

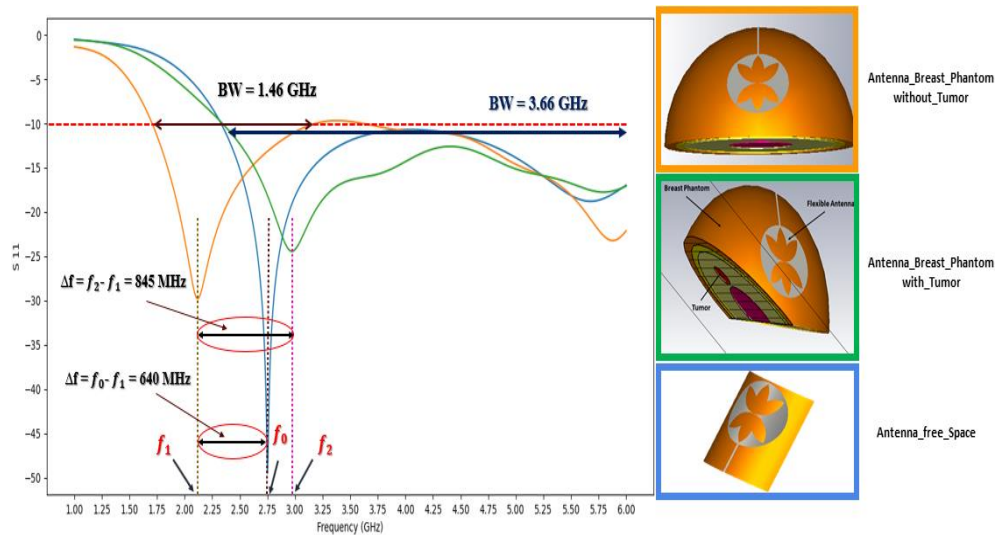


Figure 8. Results of  $S_{1,1}$  parameter for the flexible antenna positioned in free space, in contact with the healthy and abnormality of breast phantom

## 2.3. Design of the microstrip elements of the microwave radiometer front-end

### 2.3.1. Bandpass filter

This section presents the design of the first element of the microwave radiometer (see Figure 9(a)), it's a new structure of the bandpass filter realized by the microstrip technology [25], using CST MWS software (see Figure 9(b)). The resonator element is made up of segments of different lengths. The proposed filter structure is implemented on an FR-4 substrate, with relative permittivity of 4.3 and thickness ( $H_{sub}=1.6$  mm). All appropriate values for the filter parameters are presented in Table 4, from which these values have been chosen to make the filter resonate at 2.75 GHz.

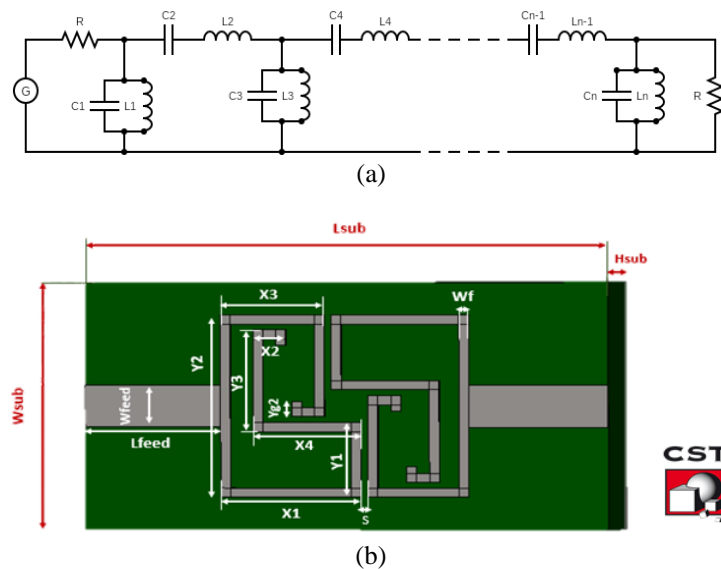


Figure 9. Bandpass filter structure for (a) equivalent circuit and (b) CST MWS model

Table 4. Microstrip bandpass filter dimensions

Parameter	$L_{sub}$	$W_{sub}$	$L_{feed}$	$W_{feed}$	$W_f$	$S$	$X_1$	$X_2$	$X_3$	$X_4$	$Y_1$	$Y_2$	$Y_3$	$Y_{g2}$
Values (mm)	16	7	4.15	2.67	0.3	0.1	4.3	1	3.2	3.3	2.43	5.91	3.3	0.5



The simulation result of the proposed filter in terms of reflection coefficient  $S_{1,1}$  and insertion loss  $S_{2,1}$  is shown in Figure 10. We can observe that the resulting bandwidth is equal to 254 MHz at a center frequency of 2.75 GHz, with the  $S_{1,1}$  of -48 dB and the  $S_{2,1}$  is equal to -0.36 dB. The positing of the two transmission zeros are situated at 2.65 GHz and 3.07 GHz, indicating a clear cutoff before and after the passband. The simulation results show that this filter has a reasonable reflection coefficient and insertion loss while offering overall filter dimensions of  $7 \times 14.8 \text{ mm}^2$ . The presented filter demonstrates a large bandwidth behavior and a fractional bandwidth (FBW) of 12%, which justifies that the proposed filter is feasible for our microwave radiometer front-end system.

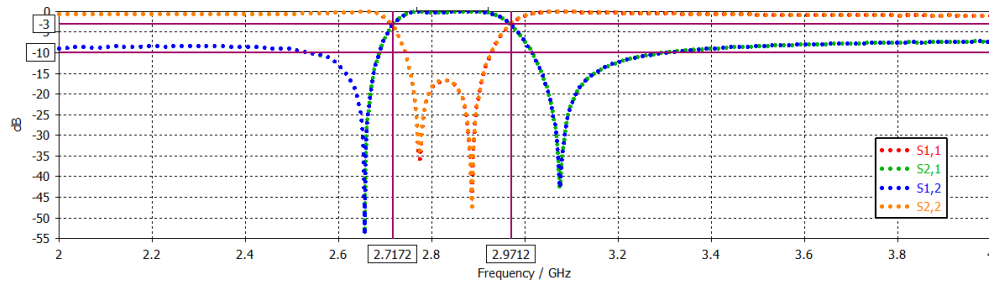


Figure 10. Return loss  $S_{1,1}$  and the insertion loss  $S_{2,1}$  of the proposed microstrip bandpass filter

### 2.3.2. Radio frequency-direct current power detector

The design of the RF-DC power detector by CST MWS is divided into three parts: schottky diode, low pass filter, and adaptation network [26]. Figure 11 shows the block diagram of the RF-DC power detector. The Table 5 compares the critical parameters for different schottky diodes. The Table 5 shows that the SMS 7630 schottky diode offers the best sensitivity for low forward powers among commercially available schottky diodes operating in the S-band. According to the studies carried out on the choice of the schottky diode, we proceeded to the modeling of its simulation program with integrated circuit emphasis (SPICE) model using CST MWS. Table 6 shows the SPICE model parameters of the SMS 7630.

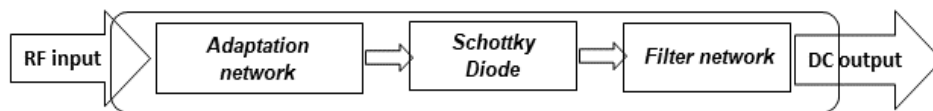


Figure 11. Functional diagram of the system

Table 5. Comparison of the characteristics of commercial schottky diodes

Diode	$V_j$ (mV)	$R_s$ (Ohms)	$C_{j0}$ (pF)	$B_V$ (V)	$I_s$ (A)
AVAGO HSMS 2860 [27]	650	6	0.18	7	$5.10^{-8}$
AVAGO HSMS 2850 [27]	350	25	0.18	3.8	$3.10^{-6}$
SKYWORKS SMS 7630 [28]	240	20	0.14	2	$5.10^{-6}$
SKYWORKS SMS 7621 [28]	510	12	0.1	3	$4.10^{-8}$

Table 6. SMS 7630 schottky diode SPICE model parameters [28]

Parameter (units)	$I_s$ (A)	$R_s$ ( $\Omega$ )	N	TT (sec)	$C_{j0}$ (pF)	M	$E_g$ (eV)	$X_{Ti}$	$F_C$	$B_V$ (V)	$I_{BV}$ (A)	$V_j$ (V)	$L_s$ (nH)	$C_P$ (pF)
Values	$5.10^{-6}$	20	1.05	$1.10^{-11}$	0.14	0.4	0.69	2	0.5	2	$1.10^{-4}$	0.51	0.05	0.005

Figure 12 shows the SPICE subcircuit model of the SMS 7630 that we developed by CST MWS. The first circuit developed is a schottky SMS 7630 diode circuit connected in series. The interest of the series diode structure is that it can detect low power levels emitted by the tumor. The substrate used is FR-4, with a thickness of  $H_{sub}=1.6 \text{ mm}$  and a relative permittivity  $\epsilon_r=4.3$ . The developed circuit has 5 blocks, namely two RF and DC filters to block higher harmonics, a schottky diode, the load, and an impedance adapter located between the RF filter and the diode, whose role is to enable maximum power transfer. Figures 13(a) and (b) show respectively, the circuit design using CST MWS and its equivalent circuit, whose RF-DC detector parameter values are mentioned in Table 7.

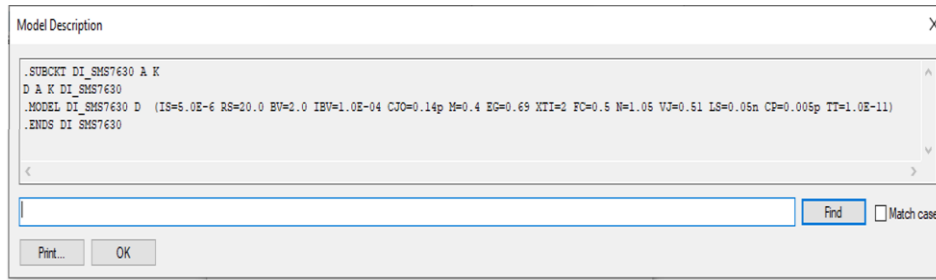


Figure 12. SPICE model of schottky diode SMS 7630 programmed using CST MWS

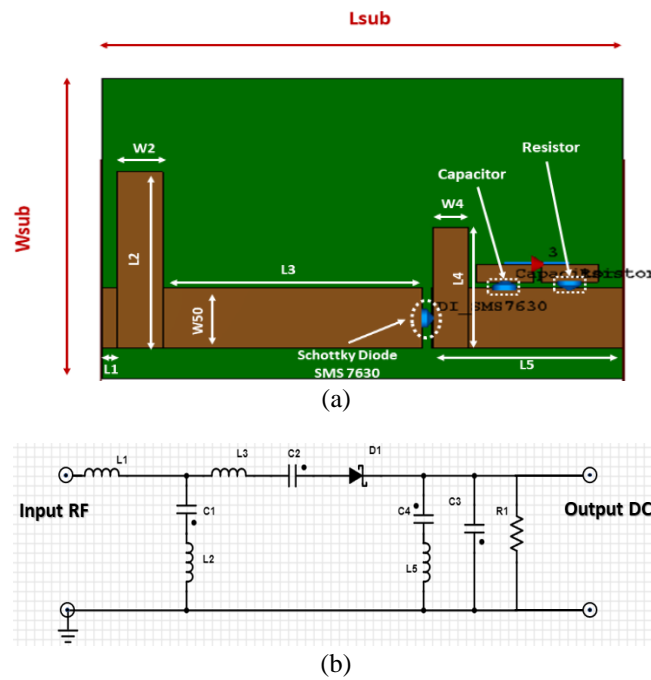


Figure 13. Structure of RF-DC power detector for; (a) CST MWS microstrip model and (b) equivalent circuit

Table 7. RF-DC power detector microstrip line parameter values

Parameter	Lsub	Wsub	L1	L2	W2	L3	W50	L4	W4	L5
Values (mm)	33.85	25	1	14.68	3	16.85	5	10.1	2.35	10

The response of RF-DC power detector (see Figures 14(a) and (b)) is optimized by using CST MWS, which corresponds to a low pass filter, whose cutoff frequency is 2.75 GHz with the rejected band varying from 2.75 GHz to 4 GHz. The result of the voltage standing wave ratio (see Figure 14(c)) is less than 2 in the frequency band (2.5-3 GHz) of the proposed detector, which shows a good improvement of the results.

### 2.3.3. Design and numerical simulation of low noise amplifier

The important aspect of the microwave radiometer is the amplification of a low-amplitude signal. Some essential elements of the amplifier design are the study of its stability. When designing an amplifier, it's important to assess the stability of an amplifier over the frequency band used. There are simpler tests to assessing the stability of an amplifier [29]. The first test is referred to the “ $K-\Delta$ ”, it provides unconditional stability if the following conditions are achieved:

$$K = \frac{1 - |S_{11}|^2 - |S_{22}|^2 + |\Delta|^2}{2|S_{12}S_{21}|} > 1 \quad (3)$$



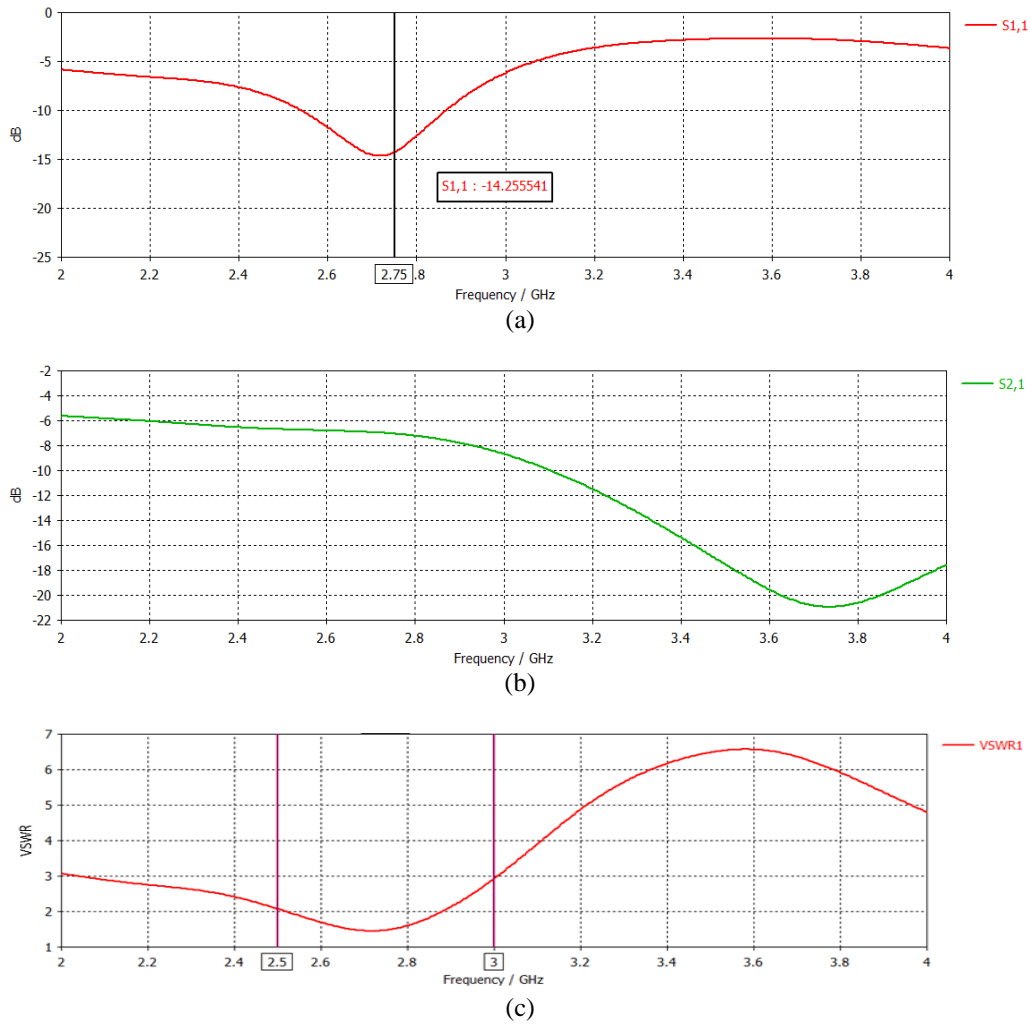


Figure 14. Simulation results for (a)  $S_{1,1}$  parameter, (b)  $S_{2,1}$  parameter, and (c) VSWR

$K$  is called Rollet's condition. Where  $\Delta$  is the determinant of the matrix  $S$ :

$$\Delta = S_{11}S_{22} - S_{12}S_{21} < 1 \quad (4)$$

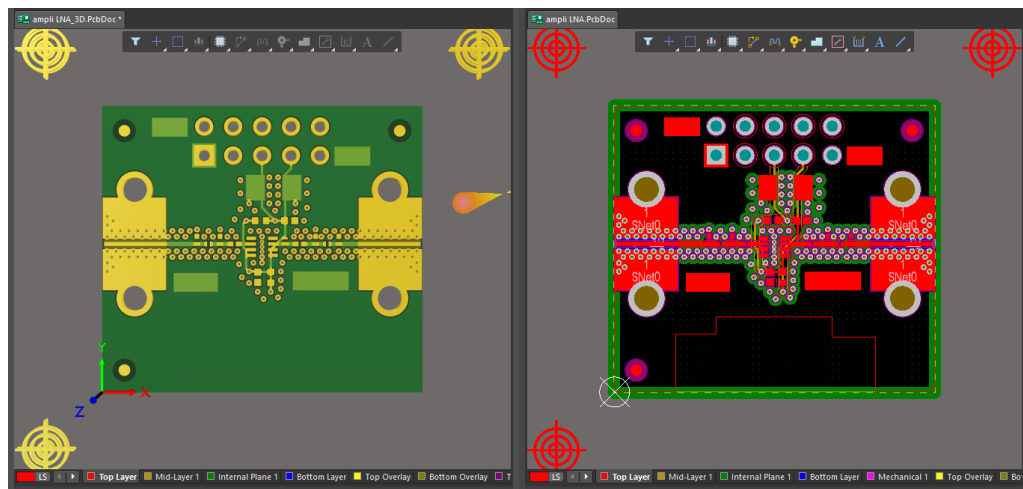
There is another criterion has been formulated, which consists a single parameter to determine the unconditional stability, namely  $\mu$ , which is defined by:

$$\mu = \frac{1 - |S_{11}|^2}{|S_{22} - \Delta S_{11}^*| + |S_{12}S_{21}|} \quad (5)$$

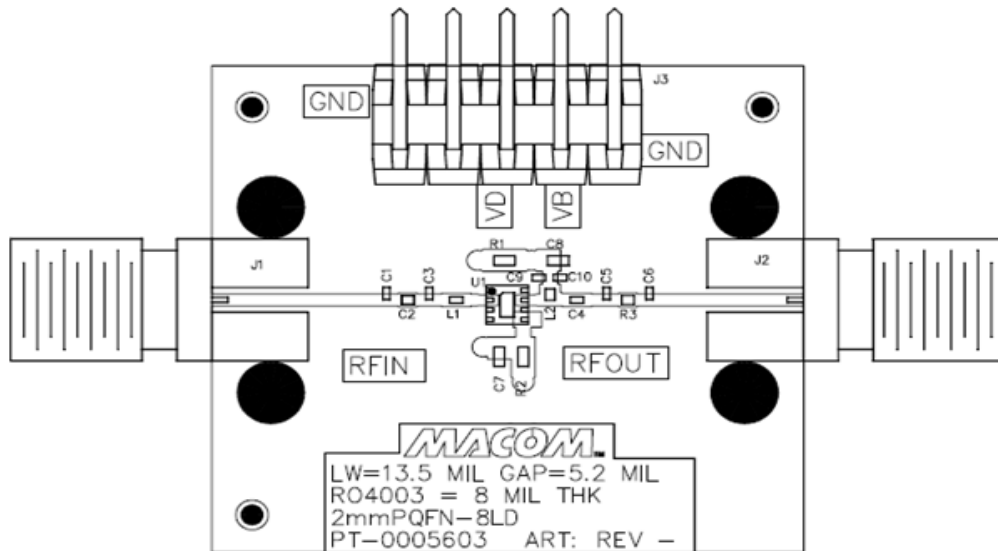
We used two software, altium designer was chosen to design the low noise amplifier bearing the reference 'MAAL-011078' (see Figure 15(a)), and CST MWS to characterize it in terms of S-parameters and stability. According to the MACOM producer of 'MAAL-011078' (see Figure 15(b)), we chose the S-parameter file with the extension '.s2p' relating to 'MAAL-011078', which we then imported into a linear array block 'touchstone' (see Figure 16).

Figures 17(a) and (b) respectively represent the simulation results of S-parameters obtained by CST MWS and those given by MACOM producer. It's quite clear that the different results obtained are identical, indeed, the gain value of 'MAAL-011078' calculated by CST MWS is 21.62 dB in the S-band, and in terms of adaptation, the  $S_{1,1}$  and  $S_{2,2}$  are always lower than -3 dB, which are similar to those given by MACOM. In terms of stability, Figure 18 presents the parameter values ( $k$ ,  $\mu$  (or  $mu$ ),  $\Delta$  (or  $delta$ )) for the MAAL-011078 component simulated using CST MWS. We notice that the MAAL-011078 respects the stability

conditions, indeed, the stability parameter  $\Delta$  is less than 1 in the S-band, and the parameters related to stability ( $k$ ,  $\mu$ ) are greater than 1 in the entire S-band.



(a)



(b)

Figure 15. Electrical circuit of 'MAAL-011078' for (a) design under altium designer and (b) dedicated by the manufacturer MACOM

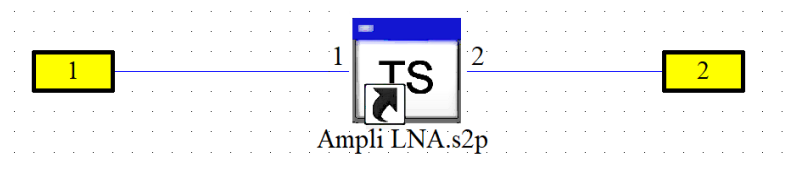


Figure 16. Touchstone block of LNA 'MAAL-011078' created using CST MWS

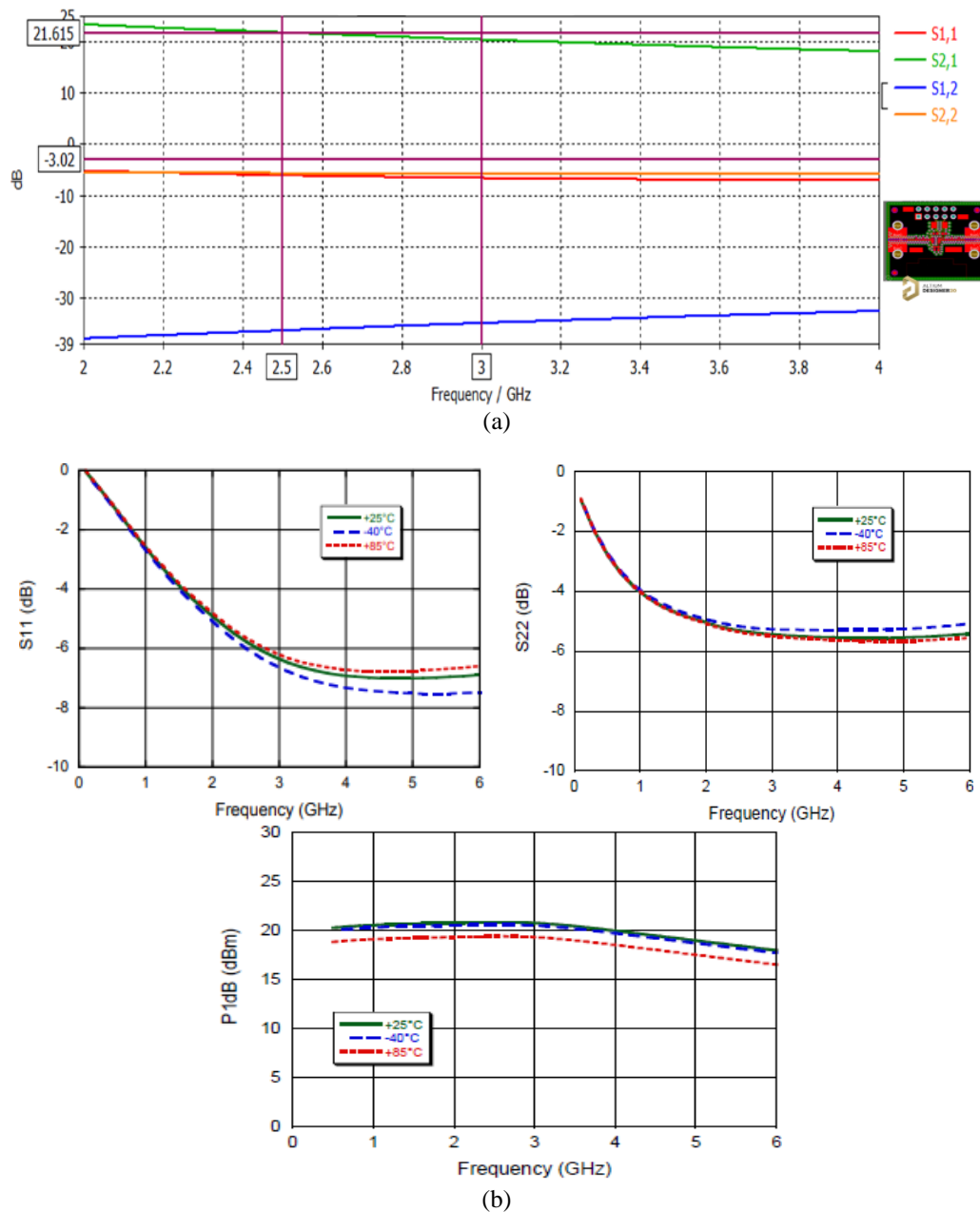


Figure 17. S-parameter results for; (a) MAAL-011078 by CST MWS and (b) dedicated by MACOM

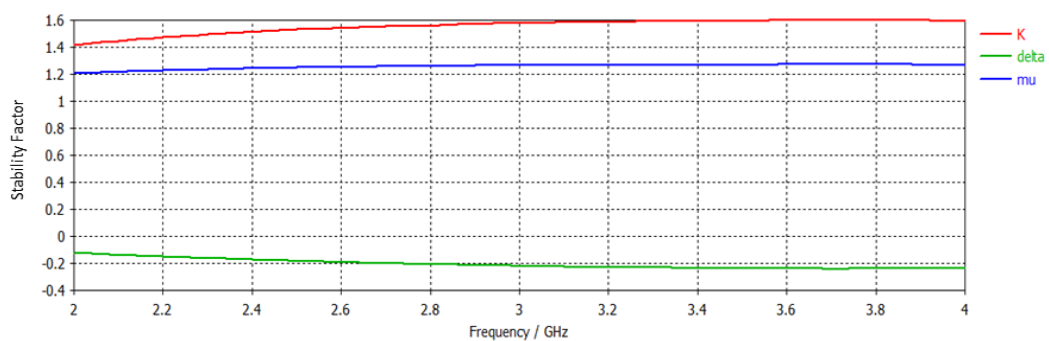


Figure 18. Stability parameters of MAAL-011078

### 3. RESULTS AND DISCUSSION

#### 3.1. Global microwave radiometer front-end system

From the simulation and interpretation results of the components designed in the previous sections, we were able to develop the global system of the radiometer front-end, associated with the normal and abnormal breast phantom, using the co-simulation modules provided by the CST MWS, as shown in Figures 19 and 20. The amplification must be quite high, for this, we used two low noise amplifiers of 'MAAL-011078' from the MACOM producer. A second-order bandpass filter presented in the previous section is inserted just after the amplifier, it delivers maximum gain in the band (2.71 to 2.97 GHz). The RF power detector is inserted as the last block, it makes it possible to convert the RF power into DC power, and to deliver the analog signal in the output of the RF radiometer front-end (port 6 and port 12) proportional to level of the noise power at the input (port 1 and port 7). In addition, this signal is proportional to the measured temperature which is then converted using an analog-to-digital converter (ADC) contained in a microcontroller, and the digital signal is then sent to the computer for processing. In this section, we inserted inside the breast phantom a mass of cancerous cells, has a diameter of 5 mm with its electrical conductivity ( $\sigma=4$  S/m as shown in Table 1) keeping the same structure of the frontal stage of the microwave radiometer presented previously.

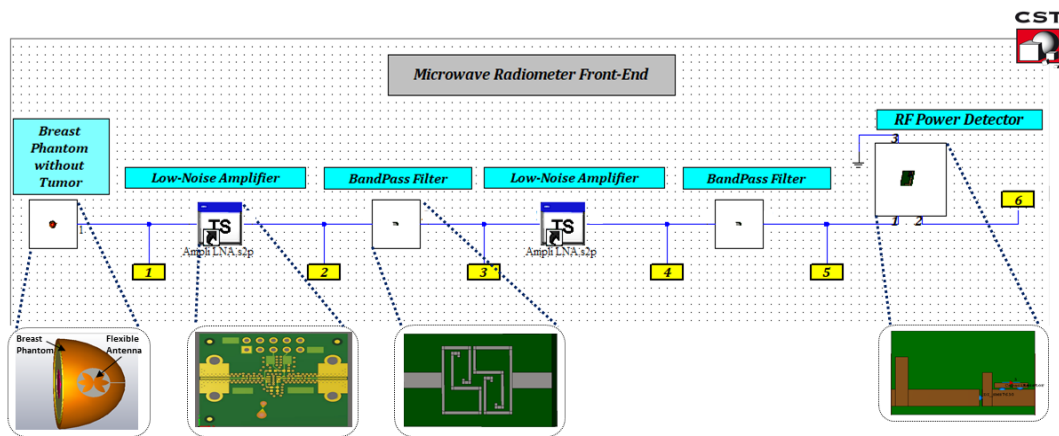


Figure 19. Co-simulation of normal breast phantom associated with the radiometer front-end part

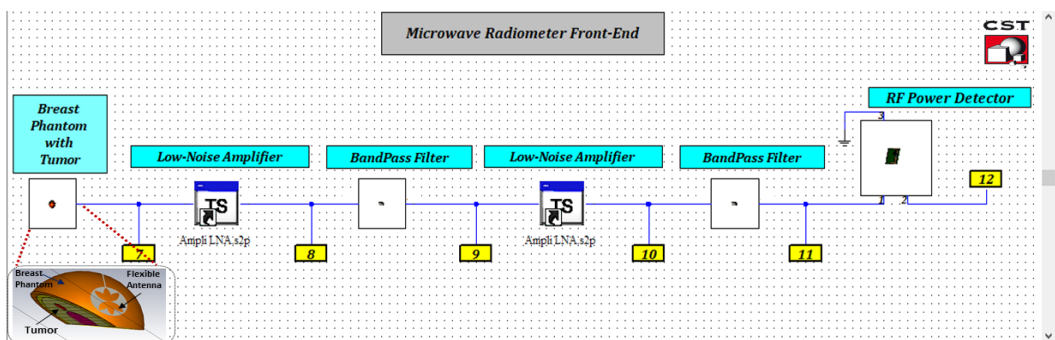


Figure 20. Co-simulation of abnormality breast phantom associated with the radiometer front-end part

#### 3.2. Interpretation of simulation results

The receiver's two most critical characteristics are gain value and the verification of its stability. Figure 21 shows the gain variation at the radiometer output for two scenarios (with and without tumor). The proposed scenarios gave the expected gain in the S-band frequency, indeed, the difference of the maximum gain  $|\Delta G_{\max}|$  measured between the abnormal and healthy phantoms is about 0.92 dB at 2.75 GHz.

Figure 22 summarizes the different simulations of the parameter's stability, we notice that the stability parameters  $\mu$  and  $k$  are greater than 1 in the S-band (see Figures 22(a) and (b)), and the delta is less than 1 (see Figure 22(c)). We can conclude that the results obtained justify the stability of the radiometer front-end associated with the breast phantom.

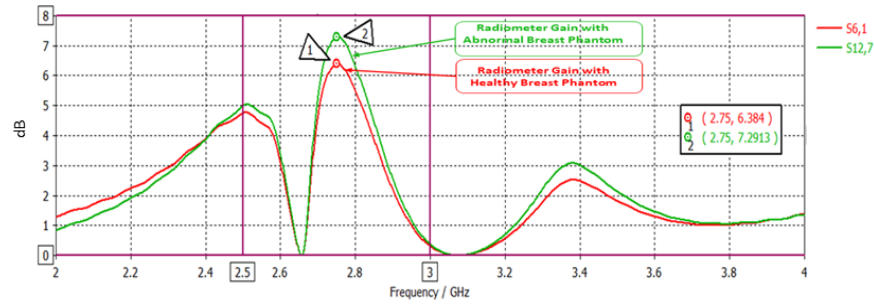
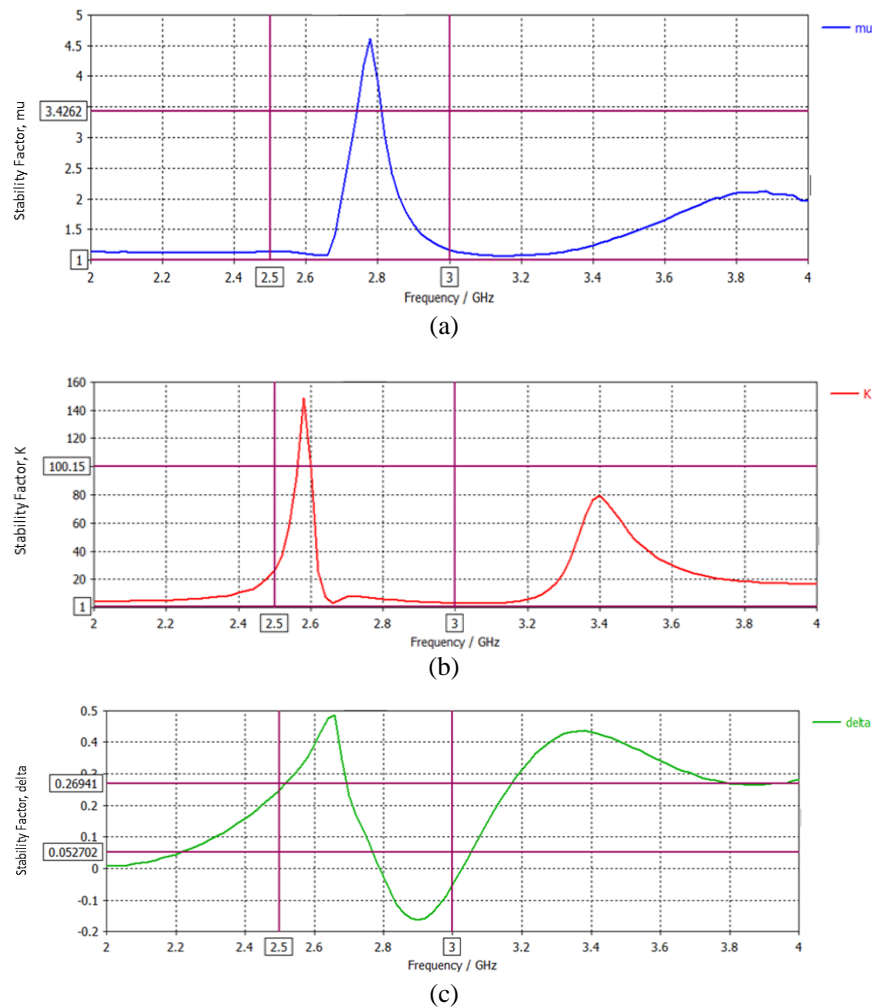


Figure 21. Gain variation measured at the output of the radiometer front-end

Figure 22. Results of stability measurements for (a) parameter  $\mu$ , (b) parameter  $\Delta$ , and (c) parameter  $K$ 

#### 4. CONCLUSION

This article describes a global study of a model of the microwave radiometric system, that is capable of detecting the presence of an anomaly inside the mammary breast, using the CST MWS simulator. We were able to study the performance and the implementation of a new miniaturized microwave radiometer for early breast cancer detection, thanks to simulations carried out on the breast phantom for both scenarios (healthy and abnormal). The results obtained from this work are satisfactory in terms of reflection/transmission coefficients, stability, and gain. For the next works, we plan to realize this system, moreover, there are two main area that may be improved in this system, firstly, due to the need for a relatively low gain, using a single amplifier is viable option, which will minimize the number of elements in the circuit and then minimize its size.

## ACKNOWLEDGEMENTS

Our research project has been selected for funding under the Al-Khawarizmi program, through a call for applied research projects in the field of artificial intelligence (AI) and its applications under the subsidy of the Ministry of Industry, Trade and Green and Digital Economy (MITGDE) in partnership with the Digital Development Agency (DDA) and the National Center for Scientific and Technical Research (CNRST).

## REFERENCES




- [1] "Breast-cancer-awareness-month-2022." [https://www-iarc-who-int.translate.goog/news-events/breast-cancer-awareness-month-2022/?\\_x\\_tr\\_sl=en&\\_x\\_tr\\_tl=fr&\\_x\\_tr\\_hl=fr&\\_x\\_tr\\_pto=sc](https://www-iarc-who-int.translate.goog/news-events/breast-cancer-awareness-month-2022/?_x_tr_sl=en&_x_tr_tl=fr&_x_tr_hl=fr&_x_tr_pto=sc) (accessed Jan. 01, 2023).
- [2] "Global Cancer Observatory." <http://globocan.iarc.fr/> (accessed Jan. 01, 2023).
- [3] J. G. Elmore, K. Armstrong, C. D. Lehman, and S. W. Fletcher, "Screening for breast cancer," *Jama*, vol. 293, no. 10, pp. 1245–1256, Mar. 2005, doi: 10.1001/jama.293.10.1245.
- [4] P. Tognolatti, R. Giusto, and F. Bardati, "A new multi-frequency microwave radiometer for medical operation," *Sensors and Actuators: A Physical*, vol. 32, no. 1–3, pp. 291–296, Apr. 1992, doi: 10.1016/0924-4247(92)80001-J.
- [5] S. V. Zinovyev, "New Medical Technology – Functional Microwave Thermography: Experimental Study," *KnE Energy*, vol. 3, no. 2, p. 547, Apr. 2018, doi: 10.18502/ken.v3i2.1864.
- [6] S. Karabetsos, G. Koulouras, P. Charamis, G. Adamidis, I. O. Vardiambasis, and A. Nassiopoulou, "Development of the RF Front-end of a Multi-Channel Microwave Radiometer for Internal Body Temperature Measurements," *Journal of Physics: Conference Series*, vol. 637, no. 1, Sep. 2015, doi: 10.1088/1742-6596/637/1/012010.
- [7] P. Momenroodaki, Z. Popovic, and R. Scheeler, "A 1.4-GHz radiometer for internal body temperature measurements," in *European Microwave Week 2015: "Freedom Through Microwaves"*, *EuMW 2015 - Conference Proceedings; 2015 45th European Microwave Conference Proceedings, EuMC*, IEEE, Sep. 2015, pp. 694–697, doi: 10.1109/EuMC.2015.7345858.
- [8] S. Shahari and A. Wakankar, "Color analysis of thermograms for breast cancer detection," in *2015 International Conference on Industrial Instrumentation and Control, ICIC 2015*, IEEE, May 2015, pp. 1577–1581, doi: 10.1109/IIC.2015.7151001.
- [9] V. P. Zharov, S. G. Vesnin, S. E. Harms, J. Y. Suen, A. V. Vaisblat, and N. Tikhomirova, "Combined interstitial laser therapy for cancer using microwave radiometric sensor and RODEO MRI feedback: I. Radio microwave," in *Laser-Tissue Interaction XII: Photochemical, Photothermal, and Photomechanical*, D. D. Duncan, S. L. Jacques, and P. C. Johnson, Eds., Jul. 2001, p. 370, doi: 10.1117/12.434722.
- [10] "CST Studio Suite Electromagnetic Field Simulation Software." <http://www.cst.com> (accessed Jan. 02, 2023).
- [11] Y. Leroy, B. Bocquet, and A. Mamouni, "Non-invasive microwave radiometry thermometry," *Physiological Measurement*, vol. 19, no. 2, pp. 127–148, May 1998, doi: 10.1088/0967-3334/19/2/001.
- [12] L. Bellarbi, M. Elkadiri, Y. Leroy, and A. Mamouni, "Temperature retrieval in lossy material by microwave correlation radiometry," *Electronics Letters*, vol. 30, no. 8, pp. 658–660, Apr. 1994, doi: 10.1049/el:19940439.
- [13] K. L. Carr, "Microwave Radiometry: Its Importance to the Detection of Cancer," *IEEE Transactions on Microwave Theory and Techniques*, vol. 37, no. 12, pp. 1862–1869, 1989, doi: 10.1109/22.44095.
- [14] Klemetsen, Y. Birkelund, S. K. Jacobsen, P. F. Maccarini, and P. R. Stauffer, "Design of medical radiometer front-end for improved performance," *Progress In Electromagnetics Research B*, vol. 27, no. 27, pp. 289–306, 2011, doi: 10.2528/PIERB10101204.
- [15] Y. Li, L. Lang, Q. Li, S. Liu, and L. Gui, "A novel Dicke microwave radiometer without temperature control for reference match load," in *9th International Conference on Microwave and Millimeter Wave Technology, ICMMT 2016 - Proceedings*, IEEE, Jun. 2016, pp. 880–882, doi: 10.1109/ICMMT.2016.7762473.
- [16] S. P. Sugumar, C. V. Krishnamurthy, and K. Arunachalam, "Characterization of microwave dicke radiometer for non-invasive tissue thermometry," in *IMBioc 2018 - 2018 IEEE/MTT-S International Microwave Biomedical Conference*, IEEE, Jun. 2018, pp. 178–180, doi: 10.1109/IMBioc.2018.8428912.
- [17] M. Planck, "On the law of distribution of energy in the normal spectrum," *Annalen der Physik*, vol. 4, 1901.
- [18] S. Singh and R. Repaka, "Parametric sensitivity analysis of critical factors affecting the thermal damage during RFA of breast tumor," *International Journal of Thermal Sciences*, vol. 124, pp. 366–374, Feb. 2018, doi: 10.1016/j.jthermalsci.2017.10.032.
- [19] A. Elouergui, L. Bellarbi, Z. Khomsi, A. Jbari, A. Errachid, and N. Yaakoubi, "A Flexible Wearable Thermography System Based on Bioheat Microsensors Network for Early Breast Cancer Detection: IoT Technology," *Journal of Electrical and Computer Engineering*, vol. 2022, pp. 1–13, Dec. 2022, doi: 10.1155/2022/5921691.
- [20] A. Channugam, R. Hatwar, and C. Herman, "Thermal analysis of cancerous breast model," in *ASME International Mechanical Engineering Congress and Exposition, Proceedings (IMECE)*, American Society of Mechanical Engineers, Nov. 2012, pp. 135–143, doi: 10.1115/IMECE2012-88244.
- [21] A. Afyf, A. Elouergui, M. Afyf, M. A. Sennouni, and L. Bellarbi, "Flexible Wearable Antenna for Body Centric Wireless Communication in S-Band," in *2020 International Conference on Electrical and Information Technologies, ICEIT 2020*, IEEE, Mar. 2020, pp. 1–4, doi: 10.1109/ICEIT48248.2020.9113217.
- [22] A. Elouergui, A. Afyf, and L. Bellarbi, "A Novel Miniaturized Circular UWB Patch Antenna: Referencing Study," in *International Conference on Multimedia Computing and Systems -Proceedings*, IEEE, May 2018, pp. 1–5, doi: 10.1109/ICMCS.2018.8525975.
- [23] A. Afyf, L. Bellarbi, A. Achour, N. Yaakoubi, A. Errachid, and M. A. Sennouni, "UWB thin film flexible antenna for microwave thermography for breast cancer detection," in *Proceedings of 2016 International Conference on Electrical and Information Technologies, ICEIT 2016*, IEEE, May 2016, pp. 425–429, doi: 10.1109/EITech.2016.7519635.
- [24] H. Absalan, A. Salmanogli, R. Rostami, and A. Maghoul, "Simulation and investigation of quantum dot effects as internal heat-generator source in breast tumor site," *Journal of Thermal Biology*, vol. 37, no. 7, pp. 490–495, Nov. 2012, doi: 10.1016/j.jtherbio.2012.05.001.
- [25] V. Miraftab and M. Yu, "Generalized lossy microwave filter coupling matrix synthesis and design using mixed technologies," *IEEE Transactions on Microwave Theory and Techniques*, vol. 56, no. 12, pp. 3016–3027, Dec. 2008, doi: 10.1109/TMTT.2008.2008267.
- [26] J. Gutiérrez, K. Zeljami, J. P. Pascual, T. Fernández, and A. Tazón, "Comparison of microstrip w-band detectors based on zero bias schottky-diodes," *Electronics (Switzerland)*, vol. 8, no. 12, Dec. 2019, doi: 10.3390/electronics8121450.
- [27] "Surface Mount Microwave Schottky Detector Diodes Data Sheet." <https://datasheet.chipsmall.com/HSMS-2860-TR1G/616733.pdf> (accessed Jul. 16, 2023).
- [28] "Data Sheet Surface-Mount Mixer and Detector Schottky Diodes." [https://www.skyworksinc.com/-/media/SkyWorks/Documents/Products/201-300/Surface\\_Mount\\_Schottky\\_Diodes\\_200041AG.pdf](https://www.skyworksinc.com/-/media/SkyWorks/Documents/Products/201-300/Surface_Mount_Schottky_Diodes_200041AG.pdf) (accessed Jan. 02, 2023).






- [29] M. L. Edwards and J. H. Sinsky, "A new criterion for linear 2-port stability using a single geometrically derived parameter," *IEEE Transactions on Microwave Theory and Techniques*, vol. 40, no. 12, pp. 2303–2311, 1992, doi: 10.1109/22.179894.

## BIOGRAPHIES OF AUTHORS






**Achraf Elouerghi**    received his master degree in Electrical Engineering from the High School of Technical Education, Rabat. Currently Ph.D. student with a research team of Electronic Systems Sensors and Nano Biotechnologies (ESSN) at ENSAM, Mohammed V University in Rabat, Morocco. His research activities are biomedical engineering, embedded systems, manufacturing engineering, radar, telecommunication systems, microelectronics, and semiconductor engineering. He can be contacted at email: achraf\_elouerghi@um5.ac.ma.






**Zakaryae Khomsi**    received his master degree in Electrical Engineering from the High School of Technical Education, Rabat. Currently Ph.D. student with a research team of Electronic Systems Sensors and Nano Biotechnologies (ESSN) at ENSAM, Mohammed V University in Rabat, Morocco. His current research interests include embedded systems, deep learning, digital electronics, embedded programming, and the internet of things. He can be contacted at email: zakaryae.khomsi95@gmail.com.



**Larbi Bellarbi**    is currently a professor at the Electrical Engineering Department of ENSAM "École Nationale Supérieure d'Arts et Métiers", Mohamed V University in Rabat, Morocco. His current research interests include electrical engineering, telecommunications engineering, electronic engineering, and embedded electronic systems. He is a member of the Electronic Systems, Sensors, and Nanobiotechnology research group. He can be contacted at email: l.bellarbi@um5r.ac.ma.



**Atman Jbari**    is currently a professor at the Electrical Engineering Department of ENSAM, Mohamed V University in Rabat, Morocco. In 2009, he received his Ph.D. in Computer and Telecommunications from Mohammed V-Agdal University. His current research interests include signal processing, blind source separation, and embedded electronic systems. He is a member of the Electronic Systems, Sensors, and Nanobiotechnology research group. He can be contacted at email: a.jbari@um5s.net.ma.